Journal of Applied Geophysics 173 (2020) 103928

Contents lists available at ScienceDirect

Journal of Applied Geophysics

journal homepage: www.elsevier.com/locate/jappgeo

Non-invasive prospection techniques and direct push sensing as high-resolution validation tools in wetland geoarchaeology – Artificial water supply at a Carolingian canal in South Germany?

Johannes Rabiger-Völlmer [a,*], Johannes Schmidt [a], Sven Linzen [b], Michael Schneider [b], Ulrike Werban [c], Peter Dietrich [c,d], Dennis Wilken [e], Tina Wunderlich [e], Annika Fediuk [e], Stefanie Berg [f], Lukas Werther [g,h], Christoph Zielhofer [a]

[a] Physical Geography, Institute of Geography, Leipzig University, Leipzig, Germany
[b] Leibniz Institute of Photonic Technology (IPHT), Jena, Germany
[c] Department Monitoring and Exploration Technologies, Helmholtz Centre for Environmental Research (UFZ), Leipzig, Germany
[d] Centre of Applied Geosciences, Eberhard Karls University, Tübingen, Germany
[e] Department of Geophysics, Institute of Geosciences, Christian-Albrechts-Universität zu Kiel, Germany
[f] Bavarian State Department for Cultural Heritage (BLfD), Munich, Germany
[g] Seminar of the Archaeology of Prehistory to the Early Middle Ages, Friedrich Schiller University, Jena, Germany
[h] Medieval Archaeology, Eberhard Karls University, Tübingen, Germany

ARTICLE INFO

Article history:
Received 17 April 2019
Received in revised form 4 October 2019
Accepted 25 December 2019
Available online 26 December 2019

Keywords:
Geoarchaeological prospection
SQUID magnetic survey
Direct push colour logs
Vibra-coring
Early Middle Ages
Fossa Carolina

ABSTRACT

The prospection of (geo-)archaeological sites yield important knowledge about the concept and the utilisation of pre-historical and historical infrastructure. The satisfactory conduction of classical prospection methods like archaeological excavations or geoarchaeological vibra-coring might be challenging in the case of large sites or difficult underground conditions. This is particularly problematic in wetlands featuring a high groundwater table and high compaction rates of organic layers.

In this study, we provide an alternative and non- to minimal-invasive exploration approach to discover hydro-engineering structures for artificial water supply in the surrounding of a Carolingian summit canal in South Germany. The Early Medieval *Fossa Carolina* was intended 792/793 CE to bridge the Central European watershed between Rhine-Main and Danube catchments. As the canal was constructed as a summit canal, an artificial water supply at the highest levels seemed very likely or even obligatory. In order to explore these obligatory hydro-engineering features, we use a wide range of on-site and off-site tools in a spatial hierarchical way. Our approach includes the large-scale SQUID magnetic survey and the sighting of historical maps. Furthermore, we integrate high-resolution direct push colour logs, and subsequent vibra-coring for small-scale stratigraphical verification and sedimentological analyses.

The SQUID magnetic survey and related depth models discover two pronounced linear anomalies that might represent potential artificial water inlets in the North-Eastern and Northern Sections of the canal. I) In the North-Eastern Section, direct push colour logs, vibra-coring and ^{14}C dating provide no evidence for a Carolingian hydro-engineering feature but reveal a natural lenticular structure of Early Holocene age. II) The linear magnetic anomaly in the Northern Section can be excluded with high probability as a hydro-engineering structure as well. Here, direct push colour logs, vibra-coring, ^{14}C dating and the comparison with a historic map reveal evidence for a historic gravel road. Thus, we have nicely verified the magnetic information but have no prove for an artificial Carolingian water inlet from the Swabian Rezat River that contradicts with assumptions of former studies.

1. Introduction

1.1. Challenging issues of archaeological excavations

Archaeological excavations of past hydro-engineering structures in wetlands can provide detailed information about buried features like construction materials, sediment type, depth and width due to an

* Corresponding author.
E-mail address: j.rabiger-voellmer@uni-leipzig.de (J. Rabiger-Völlmer).

https://doi.org/10.1016/j.jappgeo.2019.103928

exact record of the recovered stratigraphy (Schönfeld, 2009; Werther et al., 2015). However, complications are caused by deep excavation depths, high groundwater tables and unstable trench edges whereby high expenses and expenditures of time occur (Bates and Bates, 2000; Doran, 2013; Werther and Feiner, 2014). Additionally, the preservation of excavated timbers and other wooden and organic remains is difficult due to the threat of weathering under aerobe conditions (Caple, 1994). Furthermore, the results have only a selective validity on large sites.

1.2. Alternative exploration techniques and strategies

Alternatively, geoarchaeological and geotechnical prospection techniques provide a wide range of methods that are especially time- and cost-saving, non- or minimal-invasive and allow the application on different spatial scales (Boucher, 1996; Gaffney, 2008; Zielhofer et al., 2018). Techniques like magnetic prospection (Bevan and Smekalova, 2013; Schultze et al., 2008) for large-scale surveys and new direct push sensing approaches (Fischer et al., 2016; Hausmann et al., 2018; Koster, 2016; Völlmer et al., 2018) as well as vibra-coring (Leitholdt et al., 2012; Wunderlich et al., 2018) for medium to small-scale explorations become more important for geoarchaeological surveys at sites with difficult underground conditions. Here, a possibility for on-site decision making is available to modify potential investigation strategies (Döberl et al., 2012).

The application of the SQUID (Superconducting Quantum Interference Device) magnetic survey on large scales provides spatially extensive data for the localisation of underground structures in a fast way (Linzen et al., 2009; Schultze et al., 2008). For the subsurface, the application of direct push colour logs delivers unique and detailed in-situ colour information for geoarchaeological cross sections. Here, stratigraphical layers and archaeological boundaries can be identified in detail by colour contrasts (Hausmann et al., 2018). However, an important role for the validation as well as calibration plays the ground truth by vibra-coring or geoarchaeological profiling (Batayneh, 2011; Hadler et al., 2018; Köhn et al., 2019).

1.3. Geoarchaeological focus on a Carolingian canal (Fossa Carolina)

We conduct our geoarchaeological survey at the *Fossa Carolina*. The Early Medieval canal was intended to bridge the Central European watershed located at the foothills of the Southern Franconian Alb in Southern Germany (Fig. 1). The onset of the Early Medieval construction (winter 792/793 CE) is documented in written sources (Hack, 2014; Nelson, 2015) and has recently been proven by dendrochronological analysis (Werther et al., 2015). The canal is located on a valley watershed between the Swabian Rezat River in the North (Rhine-Main-Catchment) and the Altmühl River in the South (Danube-Catchment) (Fig. 2) to achieve a navigable way through Europe or rather between the North Sea and the Black Sea. The distance between the two tributaries is only approx. 2 km with a small elevation difference. Therefore, the location is very favourable for a connection canal (Leitholdt et al., 2012; Zielhofer and Kirchner, 2014).

1.4. Open questions of the canal's hydro-engineering concept

An open scientific question focuses on a probable artificial water supply for the canal. As it has been constructed with a summit level, water supply of the highest section was obligatory (Bockius, 2014;

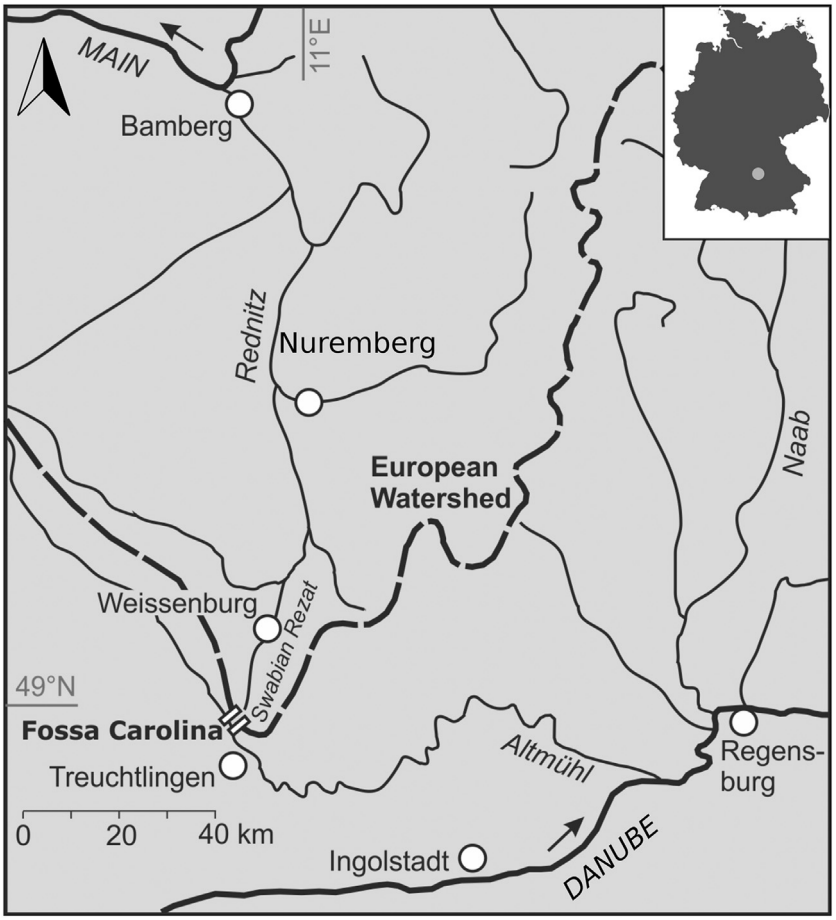

Fig. 1. Regional setting of the *Fossa Carolina*. The *Fossa Carolina* bridges the Central European Watershed between the Swabian Rezat River (Rhine-Main catchment) and the Altmühl River (Danube catchment).

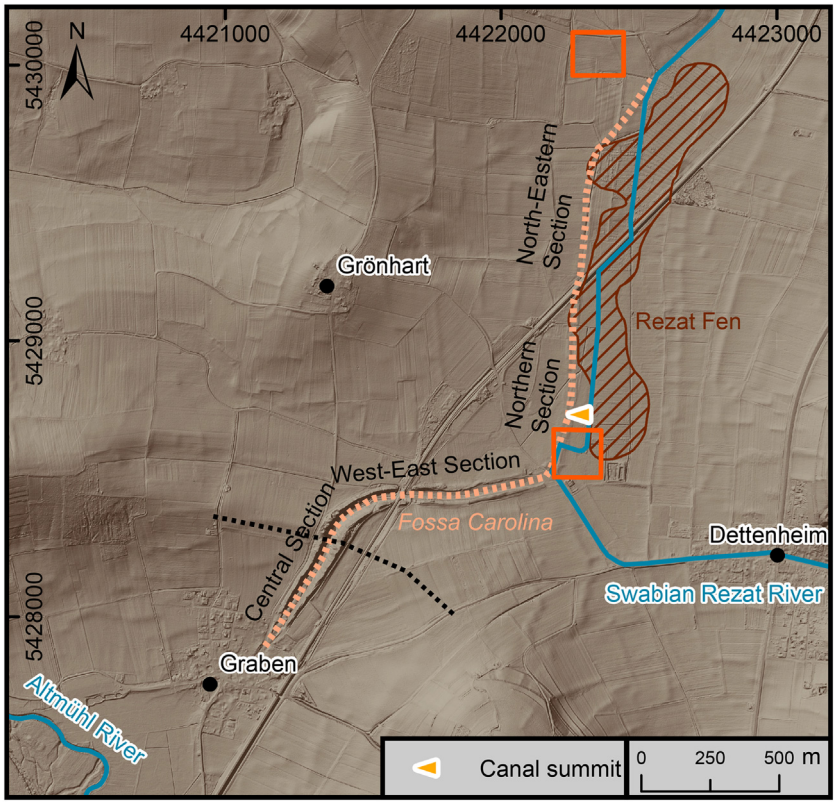

Fig. 2. Local geographical setting of the *Fossa Carolina*. The black dotted line indicates the Central European watershed. The orange dotted line indicates the course of the Carolingian canal. Major study areas are indicated by the orange squares in the North-Eastern Section and in the Northern section (Hillshade: LiDAR data are provided by Bavarian Land Surveying Office, LDBV).

Werther et al., 2018). The Swabian Rezat River (Zielhofer et al., 2014) and several smaller inlets further north are most likely to have been used for this intention. Engineers of the 19th century have intensively surveyed these possibilities (Beck, 1911; Notes du général D., 1801). Concerning the potential hydro-engineering concept of the canal, we want to prospect and clarify potential water inlet structures in the adjacent surrounding of the known canal course. To date, the potential influxes to the Carolingian summit canal are not confirmed by geoarchaeological findings.

1.5. Aim of this study

The aim of our study is to apply a spatial-hierarchical and multi-methodical approach for the prospection of archaeological features in wetlands. Our approach links information from historical maps and SQUID magnetic survey data for the prospection of hydro-engineering structures for the canal's water supply. Subsequently, we conduct high-resolution direct push colour logs on two-dimensional cross sections. The multiple colour logs will provide a depth-accurate stratigraphic information that will be the base for the selection of vibra-coring positions and the final verification or falsification of buried Carolingian water inlet structures.

2. *Fossa Carolina* - geographical and archaeological setting

2.1. Geographical setting

The landscape in the surrounding of the *Fossa Carolina* is characterised by the Jurassic Franconian escarpment landscape built from Middle Jurassic Aalenian mudstones (Dogger Alpha), Aalenian sandstones (Dogger Beta), marl and limestones (Dogger Gamma to Zeta) to Upper Jurassic limestone (Malm) (Berger and Schmidt-Kaler, 1982; Schmidt-Kaler, 1976). During the Last Glacial, the valley floors were filled with sandy to gravely deposits by enhanced fluvial dynamics. Loess was accumulated on the lower slope positions and subsequently redeposited with calcareous bedrock materials by periglacial processes (Berger and Schmidt-Kaler, 1982).

The geology affects the hydrological system. Karst fissures within the Malm carbonate rocks build hydraulic pathways. Layer boundaries within the Dogger/Malm stratigraphy cause spring horizons (e.g. spring of the Swabian Rezat River) trough clayey and marly layers of low permeability. Hydraulic effects of low permeability are visible through large Holocene fen deposits (Zielhofer and Kirchner, 2014). Discharge measurements provide additional information about the hydraulic regime within the Swabian Rezat floodplain. The results show a continuous increase of discharge by the infiltration of groundwater in the area of the Rezat Fen (Fig. 2) and might point to naturally high water availability in the area of the Northern Section of the *Fossa Carolina* (Lietz, 2014). In the surrounding of the Swabian Rezat floodplain, long term wet conditions during the Holocene are also visible by a half-bog soil, which is buried by re-deposited excavation material of the canal construction or medieval to modern flood loams (Werther et al., 2015; Zielhofer and Kirchner, 2014).

2.2. Fossa Carolina - previous (geo)archaeological findings

The results of former studies show a stepped chain of ponds as the general hydro-engineering concept for a summit canal with open waterbodies. Although the construction of the Early Medieval canal was not finished (Kirchner et al., 2018), the summit of the canal was artificially shifted approx. 1 km to the Northeast (Fig. 2) and is located close to the present Swabian Rezat River inflow (Schmidt et al., 2019; Schmidt et al., 2018; Zielhofer et al., 2014). A necessary artificial water supply (Bockius, 2014) is suspected at the highest level but not clearly proved (Werther et al., 2015). The course of the Swabian Rezat River that run into the direction of the canal at least since the 19th century

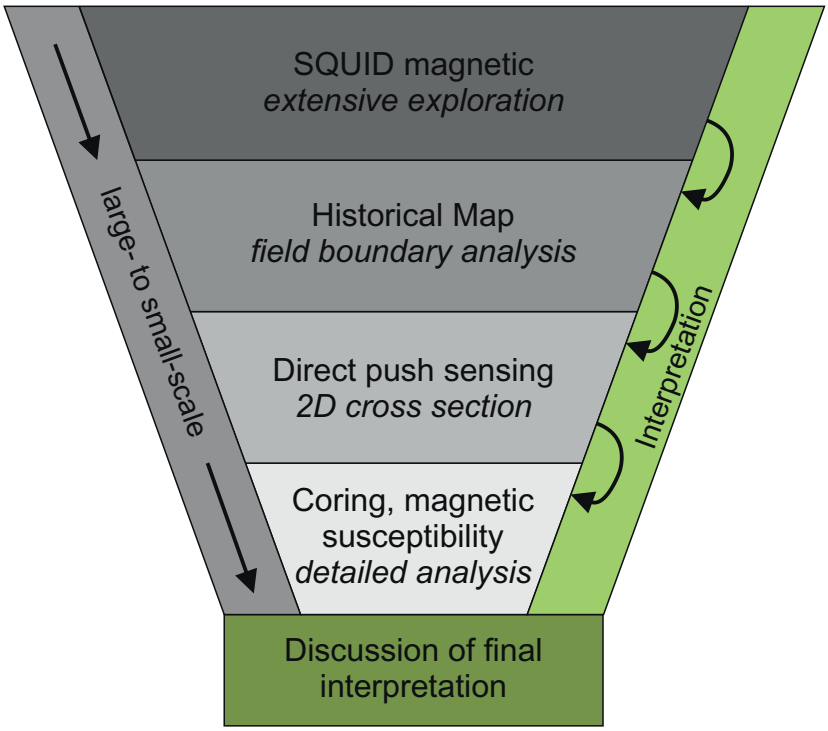

Fig. 3. Multi-methodical and hierarchical prospection approach. Concept of a spatial-hierarchical multi-methodical approach for the investigation of large (geo-)archaeological sites. The methods are conducted from large- to small-scale with intermediate interpretation steps.

leads to the hypothesis that the river was used as a Carolingian influx (Beck, 1911). However, the former assumption of an Early Medieval water storage dam (Koch, 1996) was disproved (Berg-Hobohm and Kopecky-Hermanns, 2014).

3. Methods

For the prospection, sounding and interpretation of potential Carolingian hydro-engineering structures, we conduct a hierarchical methodological approach in a spatial order from large- to small-scale (Fig. 3).

3.1. SQUID magnetic exploration

For the large-scale non-invasive prospection of linear subsurface structures, we performed magnetic surveys by means of high sensitive motorised SQUID (Superconducting Quantum Interference Device) sensors (Linzen et al., 2009). The SQUID system allows the synchronous recording of up to 12 gradiometer and 9 magnetometer signals. Thus, several components of the gradient of the Earth's magnetic field up to the full tensor can be detected. A *Matlab* script was used for post-processing and merging of all data files measured on the dozens of separated fields. Details of the general SQUID data processing can be found in Linzen et al., 2007. The magnetograms with a pixel size of 0.2×0.2 m^2 were gridded with *Surfer (Golden Software)* by use of the *Kriging* method. The maxima of magnetic information provide the possibility for the calculation of subsurface distributions of magnetic sources (Schneider et al., 2014; Schneider et al., 2013). In this way and by analogy with the magnetic anomaly of the canal itself (Linzen et al., 2017; Linzen and Schneider, 2014), several further linear and point anomalies within the prospected area are modelled. We present results of source

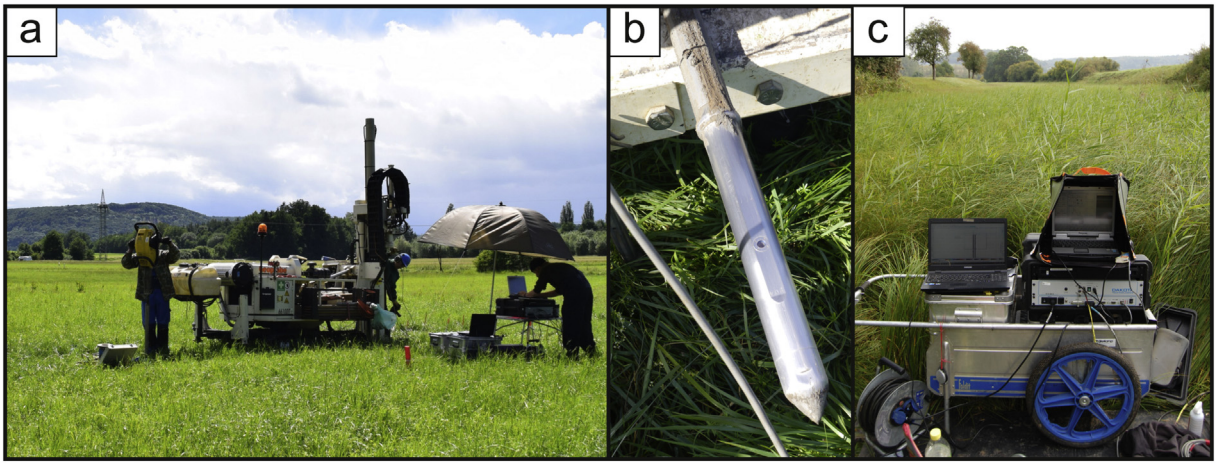

Fig. 4. Application of direct push sensing at the *Fossa Carolina*. a) Direct push sensing technique (Photo: S. Dietel 2017) equipped with b) Soil Colour Optical Screening Tool and c) equipment for on-site decision and abrupt adaption of the investigation strategy.

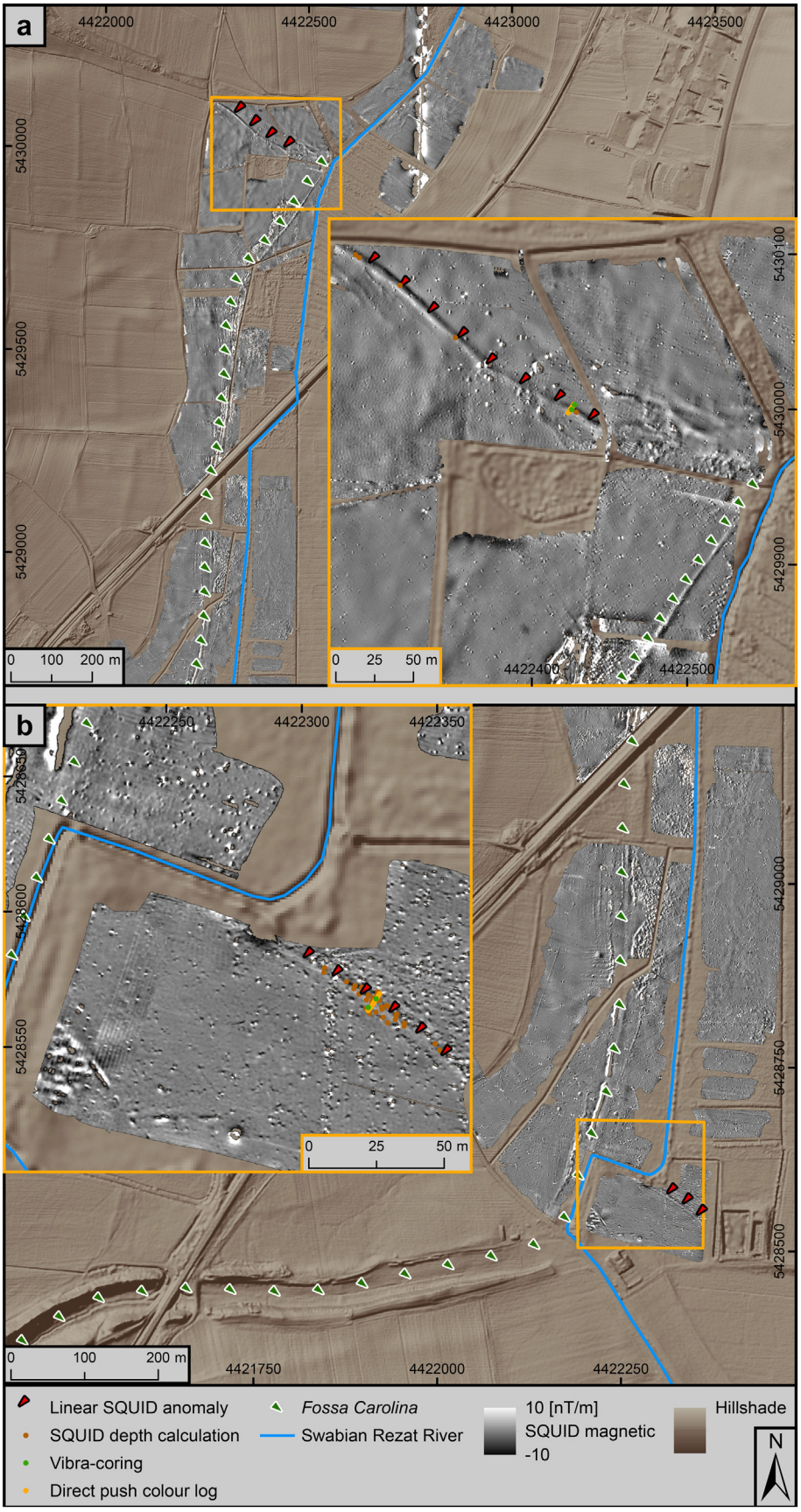

Fig. 5. SQUID-magnetic survey in the Northern-Eastern Section (a) und Northern Section (b). The red arrows mark linear structures that might correspond with a potential water inlet in the *Fossa Carolina* (green arrows). Detailed maps (yellow bordered) show vibra-coring positions (green dots), direct push colour logs (yellow dots) and positions of SQUID depth calculations (brown dots) (LiDAR data for the hillshade are provided by Bavarian Land Surveying Office, LDBV).

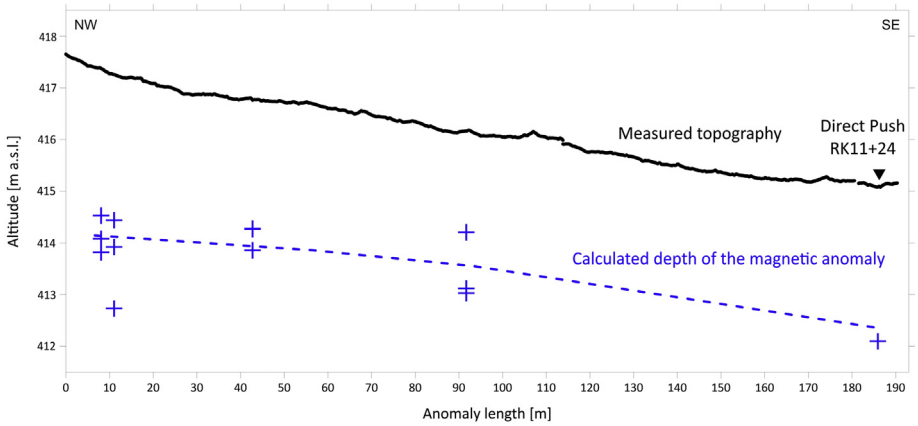

Fig. 6. Depth calculation (blue crosses) from the linear SQUID magnetic anomaly in the North-Eastern Section. The black triangle indicates the RK11 and RK24 vibra-coring positions and the direct push cross section.

depth calculations along two anomaly regions with a total length of about 240 m. The depth calculations base on fitting procedures of the original, i.e. un-gridded, measurement line data of all sensors and the assumption of dipole-like magnetic sources. The obtained depth information was combined with core and direct push analysis data.

3.2. Historical cadastral maps

The historical cadastral map (1:5000) from 1820 to 1822 (Bavarian Regional Library Online, BLO) includes older property boundaries before land consolidation was conducted in the 20th century. Thus, it reveals indices for older, pre-modern linear landscape elements like trenches that might constitute historical hydro-engineering structures (Fazioli, 2014; Kirchner et al., 2018; Smekalova et al., 2016). We used digital versions of historical cadastral maps that have been officially georeferenced by land survey authorities (Bavarian Land Surveying Office (LDBV), Version: 2012–11-206, Bayern Original maps 1820–1822).

3.3. Direct push sensing with the colour logging tool (CLT)

For the two-dimensional in-situ characterisation of underground structures and stratigraphy, we used high-resolution direct push sensing techniques. In general, steel rods with a small diameter (range 36–100 mm) and different probes are pushed or hammered in the unconsolidated underground driven by a vehicle (Bumberger et al., 2015; Dietrich and Leven, 2009; Hausmann et al., 2018; Leven et al., 2011). For our minimal-invasive investigation, we used a caterpillar (Geoprobe 6610DT) (Fig. 4) and applied the colour logging tool (CLT) (Soil Colour Optical Screening Tool, SCOST™, Dakota Technologies, Fargo, USA) with rods of 38 mm diameter. We localise each direct push position with a Topcon HiPer II DGPS. The CLT system transmits white light and logs the reflection from the sediment on a photosensitive chip in the wavelength range of 350–1000 nm. The measurements are integrated over an adjusted time interval around 300 ms for each record. The results are numerical recorded by the OST-Software (Dakota Technologies, Fargo, USA) that provides RGB data as jpg-raster images. In conjunction with the propulsion of approx. 2 cm/s, the depth resolution is in cm-scale (Dalan et al., 2011; Hausmann et al., 2016; Hausmann et al., 2013; Völlmer et al., 2018). To guarantee a consistent quality, we tested the white balance of the control unit before every probing. High friction and pressure prevent the adhesion of sediments at the probe. The field preview of the RGB colours allows on-site decision-making.

3.4. Vibra-coring

We used an Atlas Copco Cobra drilling device with open cores (diameter: 60 mm) and localised each position with a Topcon HiPer II DGPS. We describe soil horizons, Munsell colour (Munsell, 1994), grain sizes, calcareous content, hydromorphic properties and organic content (after Ad-Hoc-AG Boden, 2006) in the field. In the North-Eastern Section, we used vibra-coring within (RK11, RK24) and beside (RK10, RK25) the SQUID magnetic anomaly for stratigraphical

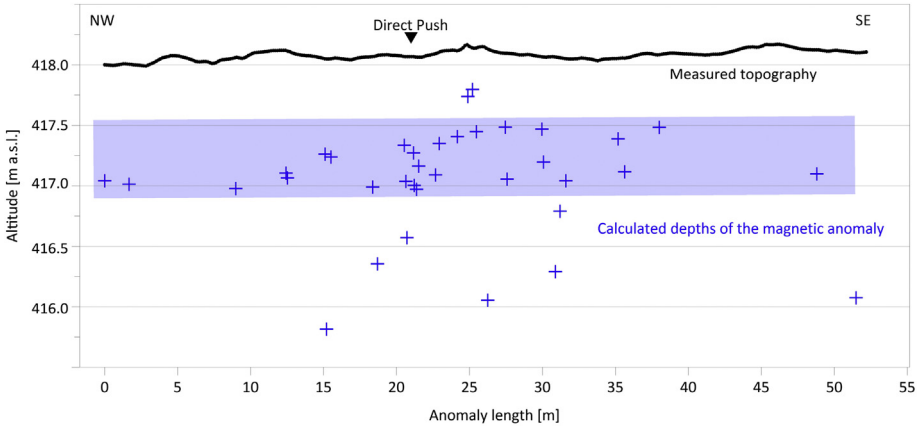

Fig. 7. Depth calculation (blue crosses) from the linear SQUID magnetic anomaly in the Northern Section. The black triangle indicates the direct push cross section.

validations and sediment sampling. The core stratigraphies of RK10 and RK11 were documented on site (after Ad-Hoc-AG Boden, 2006). For an additional magnetic susceptibility record (equidistantly 5 cm), we used the cores RK24 and RK25 from same positions as RK 11 and RK10. In the Northern section, core stratigraphies of BK1 and BK8 were documented on site (after Ad-Hoc-AG Boden, 2006). The stratigraphical data represent ground truth data for the linkage with data sets from direct push cross sections. We corrected the inaccurate depths and gaps of the core profiles with the exact depths from the direct push colour logs. Here, we converted MUNSELL colours from vibra-coring descriptions in RGB colours (Figs. 10 and 12) to allow a direct comparison of sediment core colours and direct push colour logs.

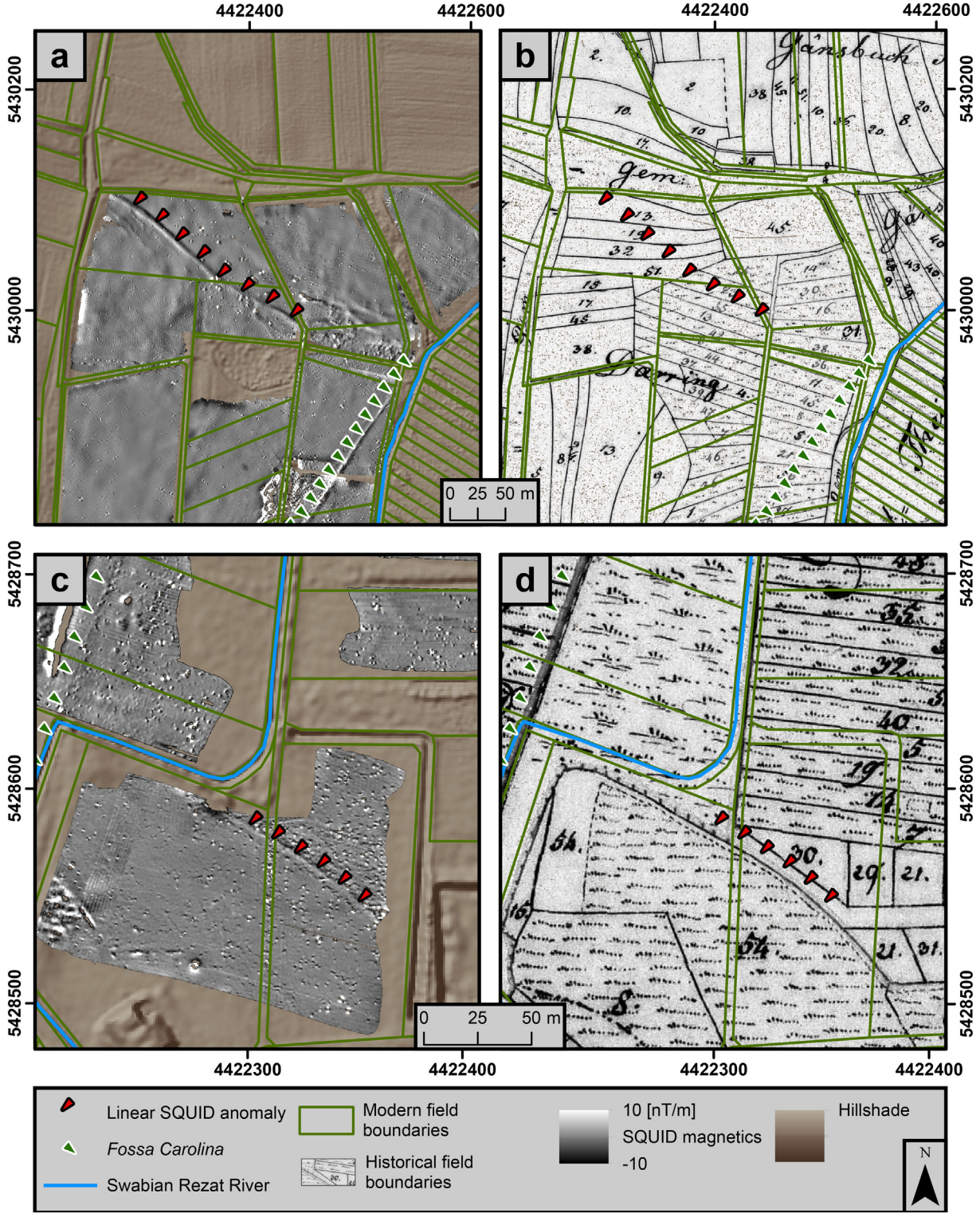

Fig. 8. Historical field boundaries might indicate historical land use, stream courses, roads or potential hydro-engineering structures. a) Magnetic anomaly in the North-Eastern Section, b) Historical cadastral map of the North-Eastern Section, c) Magnetic anomaly of the Northern Section and d) Historical cadastral map of the Northern Section (Map: Bavarian Land Surveying Office (LDBV), Cadastral map 41–20, 1820–1822; Hillshade: LiDAR data are provided by Bavarian Land Surveying Office, LDBV).

3.5. Magnetic susceptibility measurements

The mass specific magnetic susceptibility was measured at low frequency (χ_{LF}, 0.465 kHz, 10^{-6} m^3/kg). Recovered sediment samples from vibra-coring were filled in plastic boxes and measured with a Bartington MS3 based on a MS2B dual frequency sensor (Bartington Instruments, 2000) at Leipzig physical geography laboratory.

3.6. Radiocarbon dating

Wood, plant fragments and seeds were analysed with accelerator mass spectrometry (AMS) type MICADAS (Synal et al., 2007) at Klaus-Tschira-Archäometrie-Zentrum (Mannheim). The ^{14}C age calibration was conducted with the dataset INTCAL 13 (Reimer et al., 2013) and the Software SwissCal 1.0 (L. Wacker, ETH Zürich).

4. Results and Interpretation

4.1. SQUID magnetics

On the large scale, we analyse the greater geographical zone of the Carolingian canal. A first promising linear magnetic anomaly was detected in the North-Eastern Section (red arrows in Fig. 5a) that displays in detail a linear structure with a modelled depth of approx. 3 m below surface (Fig. 6). The anomaly follows a smooth depression from northwest to southeast and reaches in the lengthening the remnants of the buried Carolingian canal. The straight course of the linear anomaly and the position close to the *Fossa Carolina* lead to the assumption that it may have an anthropogenic origin that corresponds probably with a water supplying hydro-engineering structure of the Carolingian canal. Furthermore, a linear anomaly is visible in the Northern Section (red arrows in Fig. 5b) close to the course of the Swabian

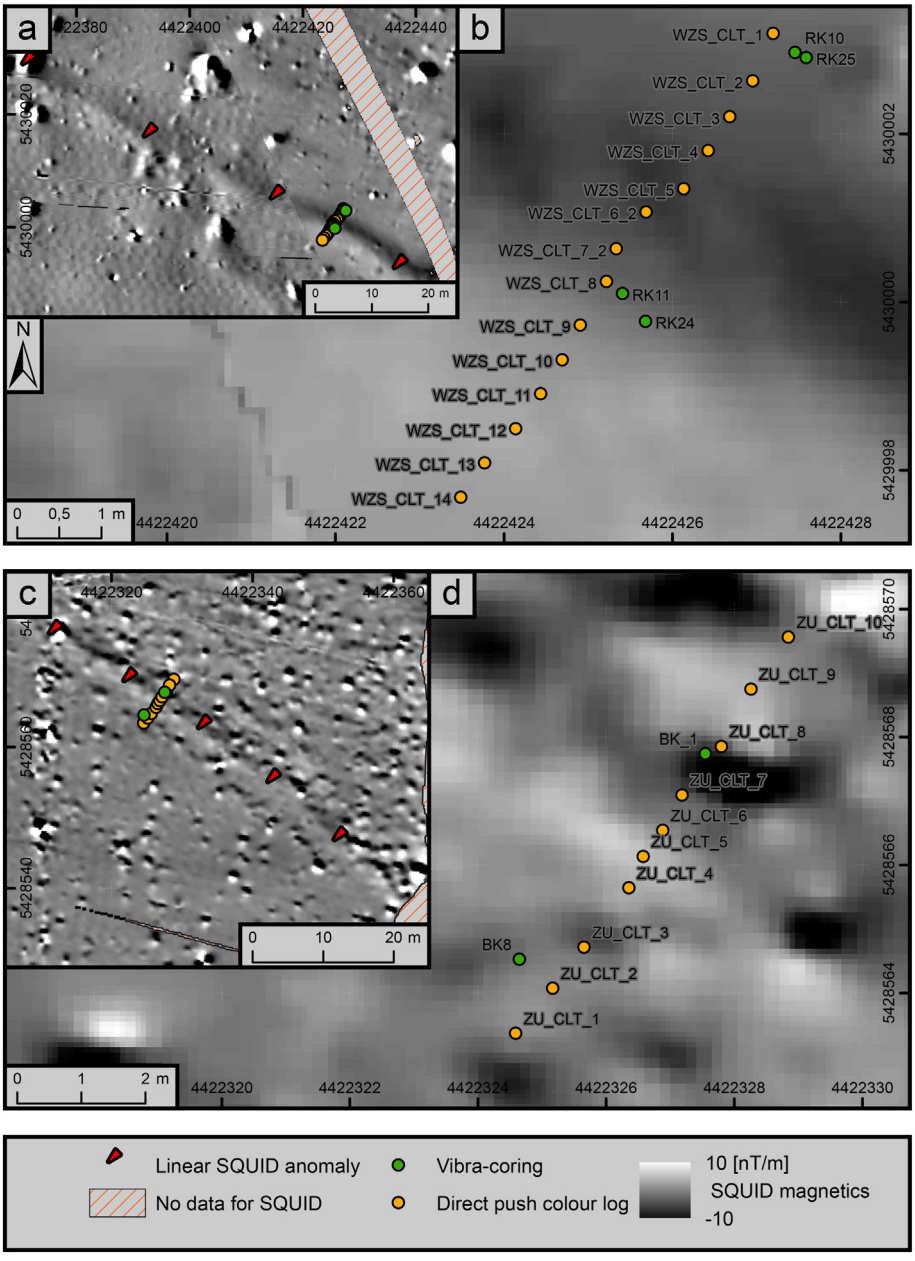

Fig. 9. Direct push cross sections and vibra-coring positions. a) North-Eastern Section with linear SQUID magnetic anomaly in the background (marked with red arrows), b) North-Eastern Section (zoomed) with direct push colour logs (yellow dots, 0.5 m spacing) and vibra-coring positions (green dots), c) Northern Section with linear SQUID magnetic anomaly in the background (marked with red arrows) and d) Northern Section (zoomed) with direct push colour logs (yellow dots, 0.5 to 1 m spacing) and vibra-coring positions (green dots).

Rezat River. The modelling of the linear magnetic anomaly clearly reveals a depth of 0.5–1 m for an entire length of about 50 m (Fig. 7: blue crosses and light-blue highlighted zone). Thus, the median anomaly depth is significantly lower than for the linear anomaly of the North-Eastern Section. However, a little number of calculations show depths of magnetic sources deeper than 2 m for the northern anomaly, too. Thus, the latter can meanly but not completely explained by near-surface objects.

4.2. Comparison with historical cadastral maps

The comparison of the two linear magnetic anomalies in North-Eastern (Fig. 8a) and Northern Sections (Fig. 8c) with historical field boundaries from around 1820 (Figs. 8b and d) shows no evidence for an overlapping in the North-Eastern Section but a clear overlapping in the Northern Section. Therefore, the magnetic anomaly in the Northern Section might correspond with a buried anthropogenic structure from the modern era, probably a pathway or road.

4.3. Direct push cross sections and vibra-coring

4.3.1. North-Eastern section

The 2D cross section (Figs. 9a, b and 10) shows high-resolution sediment colour data with a reddish brown oxidised layer below approx. 411.5 m a.s.l. (Unit I). Above, a grey to greyish brown layer (Unit II) and a lenticular yellowish brown to brown layer appear (Unit III). The latter is noticeably dipped toward southwest. A brownish yellow to brown layer (Unit IV) and a subsequent dark brown to dark yellowish brown layer (414.0 to 414.40 m a.s.l., Unit V) cover Unit III. The final layer (Unit VI) close to the surface reveals a very dark greyish brown colour.

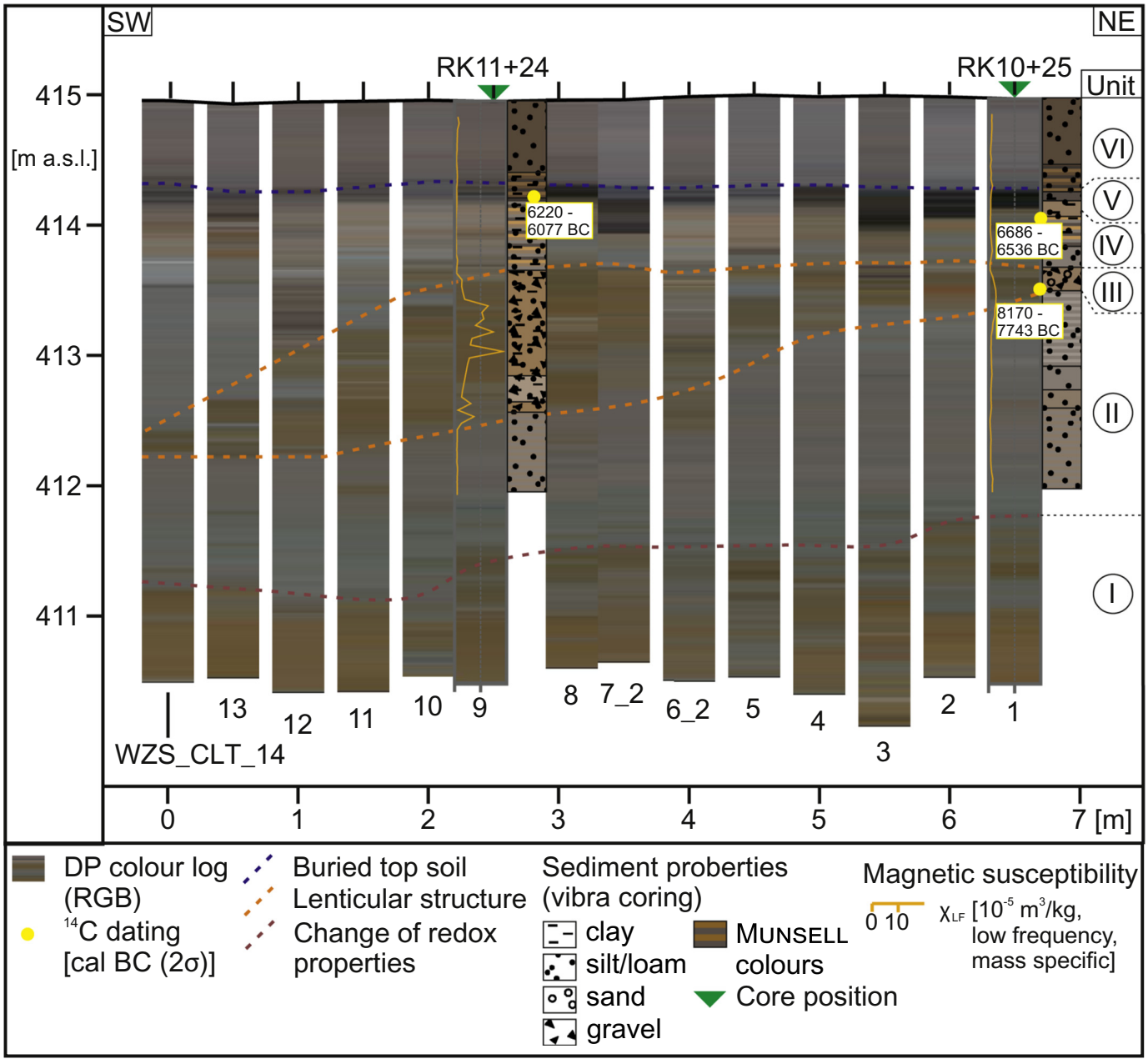

Fig. 10. Direct push cross section through the SQUID magnetic anomaly in the North-Eastern Section with direct push colour logs (WZS_CLT, 0.5 m spacing), vibra-coring positions (RK) and magnetic susceptibility values. Direct push sensing colour logs show a paleosol (414.5 m a.s.l.), a lenticular structure (Unit III) and a change of redox properties (Unit I, 411.5 m a.s.l.).

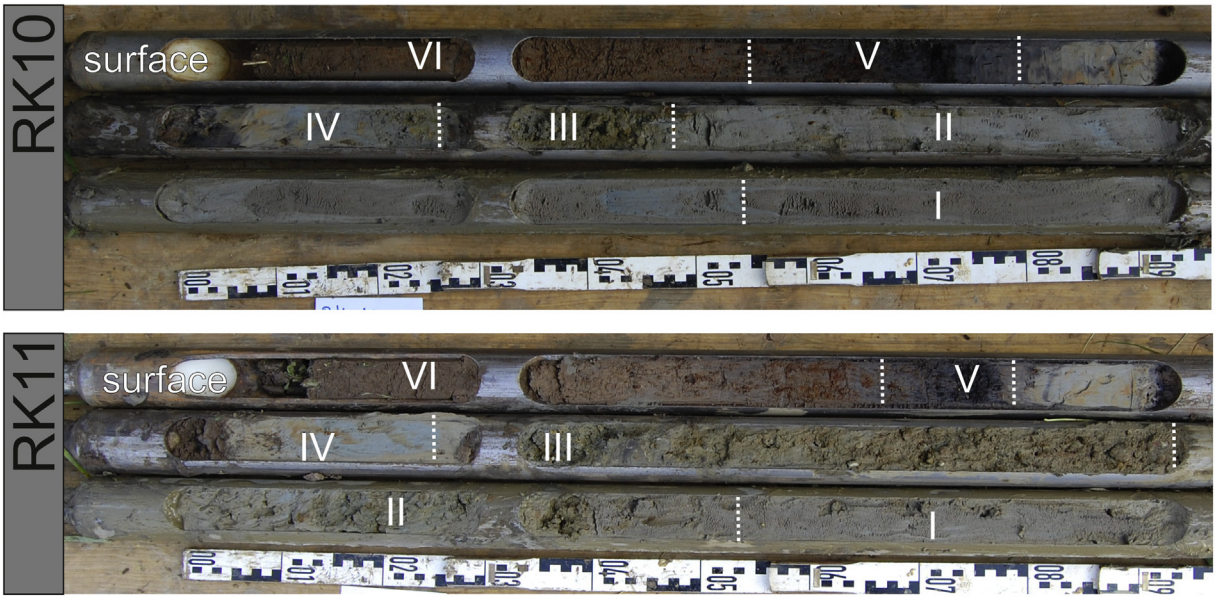

Fig. 11. RK10 (edge of anomaly) and RK11 (centre of anomaly) cores from the SQIUD magnetic anomaly in the Northern-Eastern Section. The stratigraphy shows sandy parent material (Units I and II), Early Holocene alluvial deposits from the lenticular structure (Unit III), Early Holocene alluvial sediments (Unit IV) a thin layer with a half-bog top-soil (Unit V) (Photos: J. Schmidt, 2017).

Two cores (RK 10 and 11, Figs. 10 and 11, Table 1) provide sedimentological information about the recovered stratigraphical units of the 2D direct push cross section in the North-Eastern Section. Unit II represents a clayey to sandy loam with a detectable but very low carbonate content. The following heterogeneous lenticular layer (Unit III) reveals silty clay to loamy sand with rounded gravels and few macro-plant remains. In the central part of Unit III iron and manganese oxides appear. Additionally, this layer shows significantly increased values in the mass-specific low frequency susceptibility χ_{LF}. A plant fragment at 413.56–413.38 m a.s.l. reveals an age between 8170 and 7743 cal BC (2σ) (Table 3). In the following Unit IV, the sand content decreases and the texture reveals a silty clay to sandy loam. A plant fragment at 414.17–414.14 m a.s.l. indicates an age between 6686 and 6536 cal BC (2σ) (Table 3). Subsequent Unit V consists of an organic silty clay to clayey loam. A plant fragment at 414.14–414.12 m a.s.l. indicates a calibrated age of Unit V between 6220 and 6077 cal BCE (2σ)

Table 1
North-Eastern Section - Field description of recovered cores (after Ad-Hoc-AG Boden, 2006).

Core	Unit	Layer	m a.s.l.	Depth [cm]	Colour (Munsell)		Carbonate content	Grain size	
RK10	VI	Ap	414.87–414.57	0–30	10YR 3/2	Very dark greyish brown	c0	Us2-Uls	sandy silt to loamy sandy silt
RK10	VI	rAp, M	414.57–414.36	30–51	10YR 3/2	Very dark greyish brown	c0	Uls-Ut2-Lu4	sandy loamy silt to silty loam
RK10	V	fAa	414.36–414.15	51–72	10YR 2/1, 10YR 3/3, 10YR 4/4	Black, dark brown, dark yellowish brown	c0	Lt3	clayey loam
RK10	V		414.15–414.08	72–79	10YR 3/1	Very dark grey	c0	Lt4-Tu3	clayey loam to silty clay
RK10	IV		414.08–413.96	79–91	10YR 5/3	Brown	c0	Lt4-Tu2	clayey loam to silty clay
RK10	IV		413.96–413.73	91–114	10YR 3/1, 10YR 5/1, 10YR 6/6	Very dark grey, grey, brownish yellow	c0	Lt4-Tu2	clayey loam to silty clay
RK10	IV		413.73–413.57	114–130	10YR 5/1	Grey	c0	Ls2-Ls3	loamy sand
RK10	III		413.57–413.39	130–148	10YR 5/3	Brown	c0	Ls4-Sl3 with gravels	sandy loam to loamy sand with gravels
RK10	II		413.39–412.81	148–206	10YR 6/1, 10YR 5/1	Grey, grey	c0–1	Lu3-Ls2	silty loam to sandy loam
RK10	II		412.81–412.63	206–224	10YR 5/1	Grey	c0–1	Lu3-Ls2	silty loam to sandy loam
RK10	II		412.63–412.49	224–238	10YR 5/2	Greyish brown	c0	Lu3-Ls2	silty loam to sandy loam
RK10	II		412.49–411.87	238–300	10YR 5/1, 10YR 5/2	Grey, greyish brown	c1	Lts-Lt2	clayey loam to clayey loam
RK11	VI	Ap	414.86–414.54	0–32	10YR 3/2	Very dark greyish brown	c0	Us2-Uls	sandy silt to loamy sandy silt
RK11	VI	M	414.54–414.31	32–55	10YR 3/2	Very dark greyish brown	c0	Uls-Ut2-Lu4	loamy sandy silt to clayey silt to silty loam
RK11	V	fAa	414.31–414.12	55–74.5	10YR 2/1, 10YR 3/3, 10YR 4/4	Black, dark brown, dark yellowish brown	c0	Lt4-Tu2	clayey loam to silty clay
RK11	IV		414.12–413.56	74.5–130	10YR 3/1, 10YR 5/1, 10YR 5/3, 10YR 6/6	Very dark grey, grey, brown, brownish yellow	c0	Lt4-Tu3	clayey loam to silty clay
RK11	III		413.56–412.75	130–211	10YR 5/4	Yellowish brown	c0	Lt4-Tu3 with gravels	clayey loam to silty clay with gravels
RK11	III		412.75–412.55	211–231	10YR 6/2	Light brownish grey	n.a	Lt4-Tu3 with gravels	clayey loam to silty clay with gravels
RK11	III		412.55–412.47	231–239	10YR 5/4	Yellowish brown	c0	Lt4-Tu3 with gravels	clayey loam to silty clay with gravels
RK11	II		412.47–411.86	239–300	10YR 5/1, 10YR 5/2	Grey, greyish brown	c1	Lts-Lt2	clayey loam

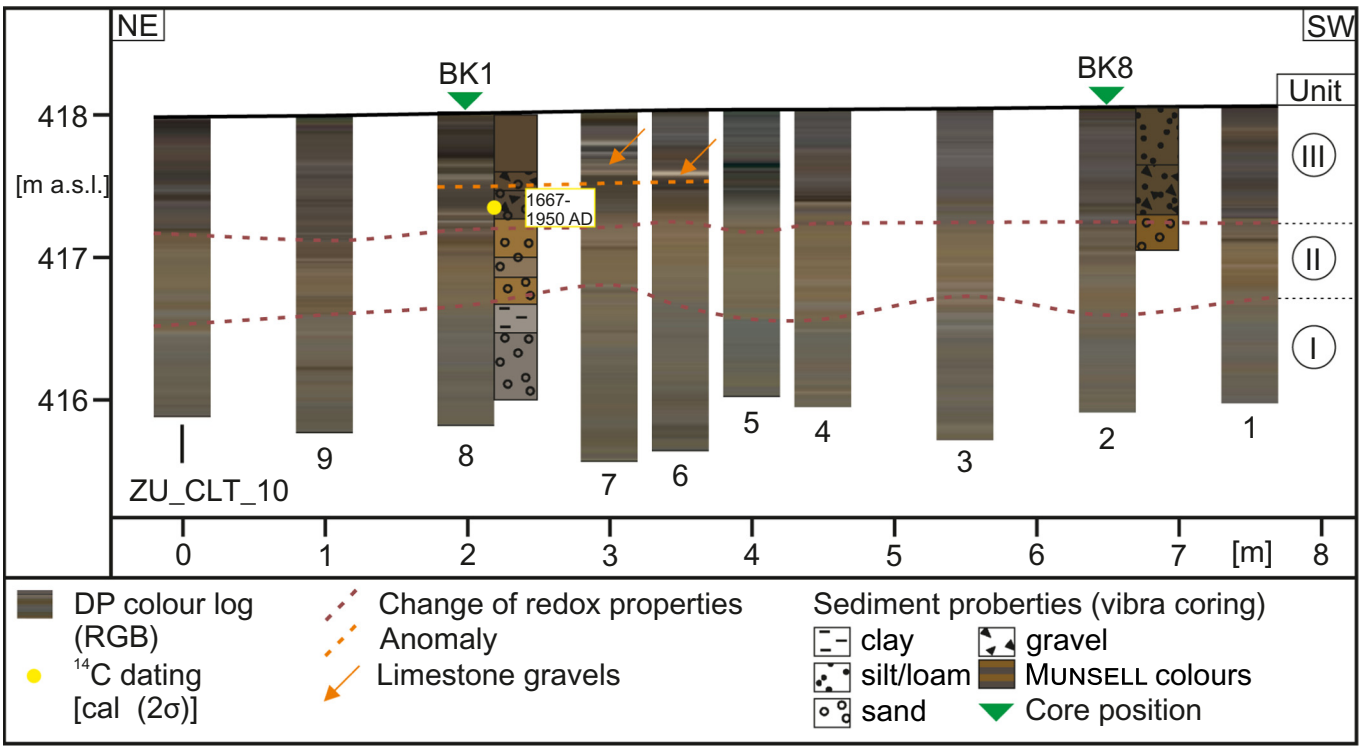

Fig. 12. Direct push cross section through the SQUID magnetic anomaly in the Northern Section with direct push colour logs (ZU_CLT, 0.5–1 m spacing) and BK vibra-coring positions. Direct push sensing colour logs show a half-bog topsoil with intercalated limestone gravels and blocks (above 417.2 m a.s.l.).

(Table 3). Clayey silts to silty loams represent the uppermost Unit VI. Further detailed sediment descriptions incl. MUNSELL colours can be found in Table 1.

We develop the following stratigraphy for the North-Eastern Section. Units I and II consist of the Pleistocene sandy-loamy parent material with changing redox properties and low calcareous contents. A special feature provides the lenticular unit (III) that represents an Early Holocene alluvial deposit. The sediment composition consists of reworked middle Jurassic (Aalenian, Dogger α) and loess deposits. The high magnetic susceptibility values indicate that Unit III caused the SQUID magnetic anomaly. An alluvial layer (Unit IV) covered the lenticular structure during the Early Holocene followed by a thin layer (Unit V) with initial half-bog soil formation (fAa). The organic-rich upper soil indicates a high groundwater table. The final Unit VI represents a flood loam from the nearby Swabian Rezat River. In general, the direct push cross section and the sedimentological data do not show a Carolingian hydro-engineering structure for artificial water supply in the North-Eastern Section.

4.3.2. Northern section

The cross section in the Northern Section (Fig. 9c+d) shows three units. The lower layers below 417.2 m a.s.l. reveal grey (Unit I) and dark yellowish brown to brown (Unit II) colours. The uppermost Unit III consists of dark olive brown to dark brown layer that is interrupted by narrow white strata (orange arrows in Fig. 12). Unit III contains gravels and fragments of limestone blocks (Fig. 13) within an organic-rich matrix. A wood remain in Unit III (417.29 m a.s.l.) reveals an age between 1667 and 1950 cal CE (2σ) (Table 3). The loamy to sandy, partially clayey texture of all units is rich in carbonates (Table 2). Following our interpretation, the profile shows a gley soil. Above

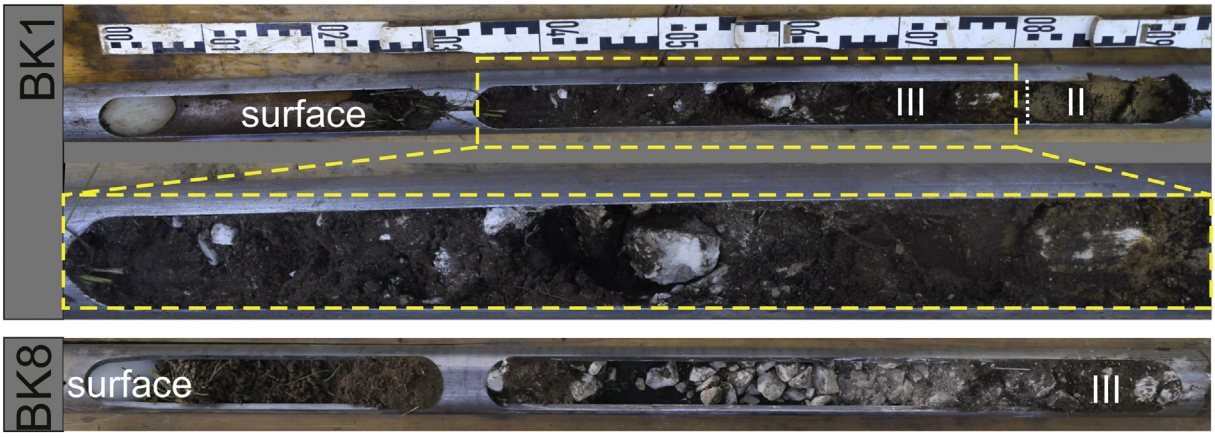

Fig. 13. BK 1 and BK 8 cores from the SQUID magnetic anomaly in the Northern Section. An organic-rich top soil matrix embeds limestone gravels and blocks. The limestones were crushed during vibra-coring (Photos: S. Dietel, 2017).

Table 2
Northern Section - Field description of recovered cores (after Ad-Hoc-AG Boden, 2006).

Core	Unit	Layer	m a.s.l.	Depth [cm]	Colour (Munsell)		Carbonate content	Grain size	
BK1	III		417.95–417.55	0–40	10YR 3/3	Dark brown	c3.4	n. a.	n. a.
BK1	III		417.55–417.42	40–53	10YR 3/3	Dark brown	c3.4	St3 with gravels	clayey sand with gravels
BK1	III		417.42–417.22	53–73	10YR 3/2	Very dark greyish brown	c3.4	St3 with gravels	loamy sand with gravels
BK1	II	Gor	417.22–416.95	73–100	10YR 5/6	Yellowish brown	c0	Sl3	loamy sand
BK1	II	Gor	416.95–416.81	100–114	10YR 5/3	Brown	c3.2	Sl3	loamy sand
BK1	II	Go	416.81–416.62	114–133	10Y2 5/6	Yellowish brown	c3.2	Sl3	loamy sand
BK1	I	Gr	416.62–416.42	133–153	10YR 6/1	Grey	c3.3	Tl	loamy clay
BK1	I	Gr	416.42–415.95	153–200	10YR 5/1	Grey	c3.2	Ss	sandy sand
BK8	III	rAp, rAh	417.98–417.58	0–40	2,5Y 3/3	Dark olive brown	c3–4	Ls3	sandy loam
BK8	III	Y?-M?	417.58–417.23	40–75	2,5Y 3/3	Dark olive brown	c3–4	Ls3 with gravels	sandy loam with gravels
BK8	II		417.23–416.98	75–100	10YR 4/6	Dark yellowish brown	c2–3	Sl2	loamy sand

417.2 m a.s.l., the dark brown colour corresponds with an increase in organic matter. The limestone blocks in the uppermost Unit III provide evidence for buried remnants of a former gravel road.

5. Discussion

5.1. Potential water-supplying hydro-engineering structures at the Fossa Carolina

Natural origin of the SQUID magnetic anomaly in the North-Eastern Section.

In the North-Eastern Section, the straight course and the depth of the SQUID magnetic anomaly is quite similar with the magnetic anomaly from the buried canal itself (Linzen et al., 2017). This might indicate a former unknown hydro-engineering structure that corresponds with the Carolingian canal construction. However, another perspective to the structure offers the detailed investigation with direct push colour logs, subsequent core analyses and ^{14}C dating. Contrary to the expected dark organic fills, which are typical for buried canal fills (Hausmann et al., 2018), the direct push colour logs of the magnetic anomaly indicate a lenticular layer (Unit III) below a half-bog topsoil (Unit V). The subsequent sediment analyses show for Unit III reworked parent rock material from the hillslope with enhanced susceptibility values that constitutes the SQUID magnetic anomaly. Radiocarbon dating provides an Early Holocene age (8170–7743 cal BCE) for the lenticular structure (Unit III), thus a geomorphological activity phase must be considered at that time. The younger ^{14}C ages (6686–6536 cal BC, 6220–-6077 cal BCE) for the buried half-bog A horizon indicate stable geomorphological conditions with a phase of semi-terrestrial soil formation. Hence, the lenticular sedimentological anomaly below the buried half-bog top soil is clearly identifiable as a pre-Carolingian structure (Fig. 10).

5.2. Hydro-engineering concept in the Northern Section

The linear SQUID magnetic anomaly in the Northern Section points to a Carolingian water inlet to the *Fossa Carolina*. Considering the nearby Swabian Rezat River, an interpretation as an artificial subsurface remain of a water inlet to the canal seems very likely. The results of the vibra-coring and from direct push sensing provide a natural layered subsurface, without organic fillings that proves the absence of a Carolingian water supplying structure. The limestone blocks indicate a pavement or a pre-modern pathway or road. The ^{14}C-dating proves the post-Carolingian age (Table 3). Hence, we find an anthropogenic structure but there is currently no evidence for a Carolingian influence.

Although earlier studies postulate for the Northern Section a reservoir for the water supply (Koch, 1996), this hypothesis has not been supported by a subsequent geoarchaeological investigation of the potential dams (Berg-Hobohm and Kopecky-Hermanns, 2014). Further, our data show that there is no detectable Carolingian drain for the water inlet of the Swabian Rezat River at the summit section of the canal. Therefore, for the hydro-engineering concept of the Northern Section might be two options possible:

I) It may be possible that water inlets have been planned but never realised because the construction site was abandoned before – such as it is very likely for the Southern connection of the canal to the Altmühl River (Kirchner et al., 2018). Furthermore, our extended survey covers a large part of the surrounding area of the canal and contains no further magnetic evidence for possible water supply features. As long as the excavation of the Carolingian canal was not finished, it would have been counterproductive to let water flow into the construction pit. As we have strong (geo-)archaeological arguments (Kirchner et al., 2018), that several sections of the canal have never been finished – as the written sources do also describe (Hack, 2014; Nelson, 2015) – it is very likely, that the intended connection to supply the summit level was not yet realised. Until the fairway was finished on the whole length, it must have been top priority to drain the groundwater from the construction pit, and not to fill it with additional water. However, there remains the possibility that we have not found the real water inlets for the canal despite the extensive survey yet. A possible reason could be low magnetic contrasts induced by different and hardly detectable trench fillings. Nevertheless, also other means of prospection such as DTM analysis (Schmidt et al., 2018), aerial archaeology (Globig, 2014) and linear archaeological excavations (Berg-Hobohm and Kopecky-Hermanns, 2014) do not offer any hints for other artificial water inlets.

II) The Rezat Fen is characterised by a high groundwater table and is almost connected with the *Fossa Carolina* in the northern summit zone as well as in the North-Eastern Section (Fig. 2). The fairway of the *Fossa Carolina* is located in depths below the groundwater table (Werther et al., 2015). Thus, the water or rather groundwater supply (Lietz, 2014; Zielhofer and Kirchner, 2014) may be sufficient for the watering of the canal and especially the summit level. Particularly,

Table 3
Radiocarbon dating. The ^{14}C age calibration was conducted with the Software SwissCal 1.0 (L. Wacker, ETH Zürich) and the INTCAL 13 (Reimer et al., 2013) dataset.

Site	Coring	Lab. No. MAMS	Depth [cm]	m a.s.l.	Location	Material	^{14}C [yr BP]	$\delta^{13}C$ AMS [‰]	cal 2σ
North-Eastern-Section	RK10	37,058	69.5–72	414.17–414.15	below fossil topsoil	peat	7798 ± 28	−17.5	6686–6536 BCE
North-Eastern-Section	RK10	37,059	130–148	413.57–413.39	alluvial material/filling	plant fragment	8809 ± 31	−19.1	8170–7743 BCE
North-Eastern-Section	RK11	37,060	72–74.5	414.14–414.12	fossil top soil	peat	7288 ± 27	−28.3	6220–6077 BCE
Northern Section	BK1	32,396	65	417.30	colluvial material/filling	wood	158 ± 22	−24.5	1667–1950 CE

Table 4
Comparison of selected exploration methods for archaeological investigations in wetlands.

	a) Method	b) Scale	c) Result configuration/ dimension	c) Depth-accuracy	d) Time expenses	e) Logistics/ fix costs	f) Method references
1) Non-invasive prospection	**Magnetometry (SQUID), vehicle driven**	**Medium to large scale**	**3D mapping (SQUID)**	**Multi-dm-scale (SQUID)**	**Low (SQUID)** to medium	**High (SQUID)**	**This study (SQUID),** Grützner et al., 2012
	Magnetometry, hand-held	Low to medium scale	2D mapping	–	Medium	Low to medium	Armstrong et al., 2019; Koivisto et al., 2018; Weston, 2001
	Electromagnetic induction survey (EMI)	Small to large scale	Cross-sections, 3D mapping	Multi-dm-scale	Low	Low to medium	Delefortrie et al., 2014; Koivisto et al., 2018; Saey et al., 2012; de Smedt et al., 2013
	Ground-penetrating radar (GPR)	Small to medium scale	Cross-sections	dm-scale	Low	Medium	Armstrong et al., 2019; Grützner et al., 2012; Howard et al., 2008; Koivisto et al., 2018
	2D Electrical resistivity tomography (ERT)	Small to medium scale	Cross-sections	dm-scale	Medium	Medium	Carey et al., 2017; Grützner et al., 2012; Howard et al., 2008
	Seismic	Small to medium scale	Cross-sections	dm-scale	Medium	Medium	Köhn et al., 2019; Verhegge et al., 2016
2) Ground truth	**DP (minimal invasive)**	**Small to medium scale**	**Cross-section, Point by point**	**cm- to dm -scale**	**Low to medium**	**High**	**This study,** Dalan et al., 2011; Hausmann et al., 2018; Missiaen et al., 2015; Völlmer et al., 2018
	Vibra Coring (minimal invasive)	**Small to medium scale**	**Cross-section, Point by point**	**dm-scale**	**Medium**	**Medium**	**This study**, Armstrong et al., 2019; Carey et al., 2017; Grützner et al., 2012; Verhegge et al., 2016
	Excavation (invasive)	Small	Cross-section, Point by point, 3D mapping	Sub-cm-scale	Very high	Medium to high	Carey et al., 2017; Grützner et al., 2012

the continuously wet conditions in the Northern Section indicate the water availability in morphological depressions also during Carolingian times. The written sources – in this particular case the revised version of the Royal Frankish Annals – do also mention that the ground was wet "by nature" (Hack, 2014; Nelson, 2015).

5.3. Combining non-invasive geophysical surveys with ground-truth data for archaeological explorations in wetlands

Non-invasive geophysical prospection techniques in wetland geoarchaeology

Non-invasive geophysical prospection techniques are suitable for local to large-scale explorations in geoarchaeology (Table 4). Some studies show a combination of different geophysical prospection techniques for comprehensive investigations (Armstrong et al., 2019; Grützner et al., 2012). In general, challenges might occur in the case of low contrasts between artefacts and surrounding sediments (Boucher, 1996; Dalan and Banerjee, 1998; Viberg et al., 2011).

At the *Fossa Carolina*, different geophysical prospection techniques were applied to detect buried canal structures in wetlands. Here, ERT cross sections indicate stratified canal fillings (Zielhofer et al., 2014) and in areas of high groundwater tables, refraction seismic and GPR cross sections show stratigraphical changes as well (Kirchner et al., 2018). However, the applied configurations of ERT, GPR and refraction seismic offer insights only on selected 2D cross sections. Thus, they are less suitable for large-scale mapping of buried geoarchaeological anomalies in the surrounding of the *Fossa Carolina* due to high time expenses. Consequently, we used the SQUID magnetic prospection technique (Table 4) that was conducted with a motorised SQUID system. This allowed prospecting an area of >120 ha in high spatial and vertical resolution within only a couple of prospection days. The recorded georeferenced magnetic maps of the *Fossa Carolina* area have a spatial resolution at cm-scale thanks to the SQUID sampling rates of 1000 measurement points per second as well as the used differential global positioning system (DGPS) and data acquisition technique. Here we can show that the data provide expressive indications with high contrasts for potential Carolingian hydro-engineering features. In wetlands, these might be caused by Greigite magnetic minerals that are formed under the impact of groundwater (Moskowitz, 1995; Roberts et al., 2011; Stele, 2017). However, not passable terrain and missing permissions to drive on the agricultural areas can handicap SQUID measurements. Alternatively, a fluxgate magnetic survey is more suitable here (Zielhofer et al., 2014).

Combined approach: Geophysical survey with required ground-truth validation techniques

In general, ground-truth techniques are required validation tools of geophysical prospection data. These in situ techniques include minimal-invasive vibra-coring, direct push sensing or invasive archaeological excavations (Table 4). The techniques provide access to sediment property information, sampling procedures and stratigraphical information about buried (geo)archaeological structures (Carey et al., 2017; Grützner et al., 2012). A common spatial hierarchical approach is the combination of large-scale geophysical surveys with point by point vibra-coring or local excavation data (e.g. Grützner et al., 2012; Keay et al., 2009). Additionally, direct push sensing in wetland archaeology provides high depth-accuracy at sites with no possibility for precise excavations and compressible sediments (Völlmer et al., 2018).

In our study, we applied a direct push colour logging tool and subsequently used vibra-coring, ^{14}C dating and magnetic susceptibility measurements to investigate two suspicious anomalies at small scale. We show that this approach (Figs. 10 and 12) allows a clear on-site falsification of potential Carolingian water inlet structures. Conducting direct push sensing and the subsequent compilation of cross sections allow the reconstruction of lithostratigraphies in high depth-accuracy that fills a gap between non-invasive geophysical exploration and selective sampling methods like vibra-coring. Furthermore, as colour-dependent features are not necessary identifiable with other geophysical methods, the sediment colour can be an excellent proxy for reconstructing buried archaeological structures in wetlands (Hausmann et al., 2018). However, a sufficient contrast of the parameter colour is necessary, similar to other geophysical parameters. Further challenges of direct push sensing can occur in case of impassable field sections as well as in the case of a highly consolidated underground.

6. Conclusions

The SQUID magnetic survey data provide two suspicious linear anomalies in the North-Eastern and Northern Sections of the *Fossa Carolina* in regard to the not finally clarified hydro-engineering concept. Additional information offer historical maps in regards to pre-modern land use. A local application of direct push sensing colour logs and vibra-coring provide high-resolution cross sections. The presented non- to minimal-invasive spatial-hierarchical multi-methodical approach shows the stepwise application of exploration techniques from large to small-scale. Our data show I) in the North-Eastern Section a buried half-bog soil horizon that represent a stable stratigraphic marker. Hence, there are no indications for a Carolingian water inlet structure. A lenticular structure below the half-bog soil horizon is part of a significant linear magnetic anomaly. However, the lenticular structure is of natural origin and of Early Holocene age. II) In the Northern Section a second linear magnetic anomaly results from limestone gravels of a buried historic road. Thus, we found no evidence for Carolingian water supplying structures. However, the subsurface aquifer from the adjacent Rezat Fen might provide enough capacity for supplying the summit of the Carolingian canal with water. Finally, the combination of large-scale SQUID magnetic survey data with small-scale direct push sending and vibra-coring offers a promising approach for a hierarchical investigation of large archaeological sites in wetlands.

Acknowledgements

For the financial support, we thank the German Research Foundation (ZI 721/12-1, HA 7419/2-1, DI 833/19-1, BE 5111/2-1) and the Bavarian State Department for Cultural Heritage (BLfD). We thank Andreas Schneider, Maximilian Bröker, Sabine Dietel and students who supported the field campaign in June 2017 (Leipzig University). For the conduction of direct push colour logs, we thank Manuel Kreck and Helko Kotas (UFZ Leipzig). For magnetic susceptibility measurements, we thank Sabine Dietel (Leipzig University). Further, we thank Anne Köhler (Leipzig University) for proofreading.

References

Armstrong, K., Cheetham, P., Darvill, T., 2019. Tales from the outer limits: Archaeological geophysical prospection in lowland peat environments in the British Isles. Archaeol. Prospect. 26 (2), 91–101. https://doi.org/10.1002/arp.1725.

Batayneh, A.T., 2011. Archaeogeophysics–archaeological prospection – a mini review. J. King Saud Univ. Sci. 23 (1), 83–89. https://doi.org/10.1016/j.jksus.2010.06.011.

Bates, M.R., Bates, C.R., 2000. Multidisciplinary Approaches to the Geoarchaeological Evaluation of deeply Stratified Sedimentary Sequences: examples from Pleistocene and Holocene Deposits in Southern England, United Kingdom. J. Archaeol. Sci. 27 (9), 845–858. https://doi.org/10.1006/jasc.2000.0584.

Beck, F., 1911. Der Karlsgraben: Eine historische, topographische und kritische Abhandlung. Verlag der Friedrich Korn'schen Buchhandlung.

Berger, K., Schmidt-Kaler, H., 1982. Geologische Karte von Bayern 6931 Weißenburg: 1:25 000.

Berg-Hobohm, S., Kopecky-Hermanns, B., 2014. Staudamm und Stausee zur Regulierung des Wasserstands in der Fossa Carolina?: Hinweise auf den holozänen Rezatverlauf. In: Ettel, P., Daim, F., Berg-Hobohm, S., Werther, L., Zielhofer, C. (Eds.), Großbaustelle 793: Das Kanalprojekt Karls des Großen zwischen Rhein und Donau. Römisch-Germanischen Zentralmuseums, Mainz, pp. 25–28.

Bevan, B.W., Smekalova, T.N., 2013. Magnetic Exploration of Archaeological Sites. In: Corsi, C. (Ed.), Good Practice in Archaeological Diagnostics: Non-invasive Survey of Complex Archaeological Sites. Springer, Cham, Heidelberg, pp. 133–152.

Bockius, R., 2014. Binnenfahrzeuge im Karolingerreich. In: Ettel, P., Daim, F., Berg-Hobohm, S., Werther, L., Zielhofer, C. (Eds.), Großbaustelle 793: Das Kanalprojekt Karls des Großen zwischen Rhein und Donau. Römisch-Germanischen Zentralmuseums, Mainz, pp. 81–86.

Ad-Hoc-AG Boden, 2006. Bodenkundliche Kartieranleitung. KA5. Schweizerbart Science Publishers, Stuttgart.

Boucher, A.R., 1996. Archaeological feedback in geophysics. Archaeol. Prospect. 3 (3), 129–140. https://doi.org/10.1002/(SICI)1099-0763(199609)3:3<129:AID-ARP49>3.0.CO;2-#.

Bumberger, J., Paasche, H., Dietrich, P., 2015. Systematic description of direct push sensor systems: a conceptual framework for system decomposition as a basis for the optimal sensor system design. J. Appl. Geophys. 122, 210–217. https://doi.org/10.1016/j.jappgeo.2015.06.003.

Caple, C., 1994. Reburial of waterlogged wood, the problems and potential of this conservation technique. Int. Biodeterior. Biodegradation 34 (1), 61–72. https://doi.org/10.1016/0964-8305(94)90020-5.

Carey, C., Howard, A.J., Jackson, R., Brown, A., 2017. Using geoarchaeological deposit modelling as a framework for archaeological evaluation and mitigation in alluvial environments. J. Archaeol. Sci. Rep. 11, 658–673. https://doi.org/10.1016/j.jasrep.2017.01.013.

Dalan, R.A., Banerjee, S.K., 1998. Solving archaeological problems using techniques of soil magnetism. Geoarchaeology 13 (1), 3–36. https://doi.org/10.1002/(SICI)1520-6548(199801)13:1<3:AID-GEA2>3.0.CO;2–9.

Dalan, R.A., Bevan, B.W., Goodman, D., Lynch, D., de Vore, S., Adamek, S., Martin, T., Holley, G., Michlovic, M., 2011. The Measurement and Analysis of Depth in Archaeological Geophysics: Tests at the Biesterfeldt Site, USA. Archaeol. Prospect. 18 (4), 245–265. https://doi.org/10.1002/arp.419.

de Smedt, P., van Meirvenne, M., Herremans, D., de Reu, J., Saey, T., Meerschman, E., Crombé, P., de Clercq, W., 2013. The 3-D reconstruction of medieval wetland reclamation through electromagnetic induction survey. Sci. Rep. 3, 1517. https://doi.org/10.1038/srep01517.

Delefortrie, S., Saey, T., van de Vijver, E., de Smedt, P., Missiaen, T., Demerre, I., van Meirvenne, M., 2014. Frequency domain electromagnetic induction survey in the intertidal zone: Limitations of low-induction-number and depth of exploration. J. Appl. Geophys. 100, 14–22. https://doi.org/10.1016/j.jappgeo.2013.10.005.

Dietrich, P., Leven, C., 2009. Direct push-technologies. In: Kirsch, R. (Ed.), Groundwater Geophysics: A Tool for Hydrogeology, 2nd ed Springer, Berlin, pp. 347–366.

Döberl, G., Müller, D., Dörrie, T., 2012. Guideline: Section 1. In: Kästner, M., Braeckevelt, M., Döberl, G., Cassiani, G., Papini, M.P., Leven-Pfister, C., van Ree, D. (Eds.), Model-Driven Soil Probing, Site Assessment and Evaluation: Guidance on Technologies. Sapienza Universita Editrice, Rom.

Doran, G.H., 2013. Excavating wet sites. In: Menotti, F., O'Sullivan, A. (Eds.), The Oxford Handbook of Wetland Archaeology, 1st ed Oxford Univ. Press, Oxford, pp. 483–494.

Fazioli, K.P., 2014. A Multidisciplinary Approach to medieval and early Modern Land Use: a Case Study from Southeastern Austria. Archaeol. Prospect. 21 (4), 235–244. https://doi.org/10.1002/arp.1485.

Fischer, P., Wunderlich, T., Rabbel, W., Vött, A., Willershäuser, T., Baika, K., Rigakou, D., Metallinou, G., 2016. Combined Electrical Resistivity Tomography (ERT), Direct-push Electrical Conductivity (DP-EC) Logging and Coring - a New Methodological Approach in Geoarchaeological Research. Archaeol. Prospect. 23 (3), 213–228. https://doi.org/10.1002/arp.1542.

Gaffney, C., 2008. Detecting Trends in the Prediction of the buried past: a Review of Geophysical Techniques in Archaeology. Archaeometry 50 (2), 313–336. https://doi.org/10.1111/j.1475-4754.2008.00388.x.

Globig, P., 2014. Luftbildarchäologische Untersuchungen im Umfeld des Karlsgrabens: (unpublished bachlor thesis). Seminar of the Archaeology of Prehistory to the Early Middle Ages. Friedrich Schiller University.

Grützner, C., Bemmann, J., Berking, J., Frechen, M., Klinger, R., Klitzsch, N., Linzen, S., Mackens, S., Oczipka, M., Piezonka, H., Reichert, S., Schneider, M., Schütt, B., 2012. Improving archaeological site analysis: a rampart in the middle Orkhon Valley investigated with combined geoscience techniques. J. Geophys. Eng. 9 (4), S70–S80. https://doi.org/10.1088/1742-2132/9/4/S70.

Hack, A., 2014. Der Bau des Karlsgrabens nach den Schriftquellen. In: Ettel, P., Daim, F., Berg-Hobohm, S., Werther, L., Zielhofer, C. (Eds.), Großbaustelle 793: Das Kanalprojekt Karls des Großen zwischen Rhein und Donau. Römisch-Germanischen Zentralmuseums, Mainz, pp. 53–62.

Hadler, H., Vött, A., Newig, J., Emde, K., Finkler, C., Fischer, P., Willershäuser, T., 2018. Geoarchaeological evidence of marshland destruction in the area of Rungholt, present-day Wadden Sea around Hallig Südfall (North Frisia, Germany), by the Grote Mandrenke in 1362 AD. Quat. Int. 473, 37–54. https://doi.org/10.1016/j.quaint.2017.09.013.

Hausmann, J., Steinel, H., Kreck, M., Werban, U., Vienken, T., Dietrich, P., 2013. Two-dimensional geomorphological characterization of a filled abandoned meander using geophysical methods and soil sampling. Geomorphology 201, 335–343. https://doi.org/10.1016/j.geomorph.2013.07.009.

Hausmann, J., Dietrich, P., Vienken, T., Werban, U., 2016. Technique, analysis routines, and application of direct push-driven in situ color logging. Environ. Earth Sci. 75 (11). https://doi.org/10.1007/s12665-016-5515-7.

Hausmann, J., Zielhofer, C., Werther, L., Berg-Hobohm, S., Dietrich, P., Heymann, R., Werban, U., 2018. Direct push sensing in wetland (geo)archaeology: High-resolution reconstruction of buried canal structures (Fossa Carolina , Germany). Quat. Int. 473, 21–36. https://doi.org/10.1016/j.quaint.2017.02.008.

Howard, A.J., Brown, A.G., Carey, C.J., Challis, K., Cooper, L.P., Kincey, M., Toms, P., 2008. Archaeological resource modelling in temperate river valleys: a case study from the Trent Valley, UK. Antiquity 82 (318), 1040–1054. https://doi.org/10.1017/S0003598X00097763.

Bartington Instruments, 2000. MS3 Magnetic Susceptibility Meter.

Keay, S., Earl, G., Hay, S., Kay, S., Ogden, J., Strutt, K.D., 2009. The role of integrated geophysical survey methods in the assessment of archaeological landscapes: the case of Portus. Archaeol. Prospect. 16 (3), 154–166. https://doi.org/10.1002/arp.358.

Kirchner, A., Zielhofer, C., Werther, L., Schneider, M., Linzen, S., Wilken, D., Wunderlich, T., Rabbel, W., Meyer, C., Schmidt, J., Schneider, B., Berg-Hobohm, S., Ettel, P., 2018. A multidisciplinary approach in wetland geoarchaeology: survey of the missing southern canal connection of the Fossa Carolina (SW Germany). Quat. Int. 473, 3–20.

Koch, R., 1996. Neue Beobachtungen und Forschungen zum Karlsgraben. 97. Jahrbuch des historischen Vereins für Mittelfranken 1–16.

Köhn, D., Wilken, D., de Nil, D., Wunderlich, T., Rabbel, W., Werther, L., Schmidt, J., Zielhofer, C., Linzen, S., 2019. Comparison of time-domain SH waveform inversion strategies based on sequential low and bandpass filtered data for improved

resolution in near-surface prospecting. J. Appl. Geophys. 160, 69–83. https://doi.org/10.1016/j.jappgeo.2018.11.001.
Koivisto, S., Latvakoski, N., Perttola, W., 2018. Out of the Peat: preliminary Geophysical Prospection and Evaluation of the Mid-Holocene Stationary Wooden Fishing Structures in Haapajärvi, Finland. J. Field Archaeol. 43 (3), 166–180. https://doi.org/10.1080/00934690.2018.1437315.
Koster, K., 2016. Cone penetration testing: a sound method for urban archaeological prospection. Archaeological Prospection 23 (1), 55–69. https://doi.org/10.1002/arp.1531.
Leitholdt, E., Zielhofer, C., Berg-Hobohm, S., Schnabl, K., Kopecky-Hermanns, B., Bussmann, J., Härtling, J.W., Reicherter, K., Unger, K., 2012. Fossa Carolina: the first Attempt to Bridge the central European Watershed-a Review, New Findings, and Geoarchaeological challenges. Geoarchaeology 27 (1), 88–104. https://doi.org/10.1002/gea.21386.
Leven, C., Weiß, H., Vienken, T., Dietrich, P., 2011. Direct-Push-Technologien – Effiziente Untersuchungsmethoden für die Untergrunderkundung. Grundwasser 16 (4), 221–234. https://doi.org/10.1007/s00767-011-0175-8.
Lietz, K., 2014. Hydrogeochemische Analyse des Einzugsgebietes der Schwäbischen Rezat im Siechten Karst der Südlichen Frankenalb: (unpublished master thesis). Institute of Geography, Leipzig University.
Linzen, S., Schneider, M., 2014. Der Karlsgraben im Fokus der Geophysik. In: Ettel, P., Daim, F., Berg-Hobohm, S., Werther, L., Zielhofer, C. (Eds.), Großbaustelle 793: Das Kanalprojekt Karls des Großen zwischen Rhein und Donau. Römisch-Germanischen Zentralmuseums, Mainz, pp. 29–32.
Linzen, S., Chwala, A., Schultze, V., Schulz, M., Schüler, T., Stolz, R., Bondarenko, N., Meyer, H.-G., 2007. A LTS-SQUID System for Archaeological Prospection and its Practical Test in Peru. IEEE Trans. Appl. Supercond. 17 (2), 750–755. https://doi.org/10.1109/TASC.2007.898570.
Linzen, S., Schultze, V., Chwala, A., Schüler, T., Schulz, M., Stolz, R., Meyer, H.-G., 2009. Quantum Detection Meets Archaeology – Magnetic Prospection with SQUIDs, Highly Sensitive and Fast. In: Herrmann, B., Reindel, M., Wagner, G.A. (Eds.), New Technologies for Archaeology: Multidisciplinary Investigations in Palpa and Nasca, Peru. Springer Berlin Heidelberg, Berlin, Heidelberg, pp. 71–85.
Linzen, S., Schneider, M., Berg-Hobohm, S., Werther, L., Ettel, P., Zielhofer, C., Schmidt, J., Fassbinder, J.W.E., Wilken, D., Fediuk, A., Dunkel, S., Stolz, R., Meyer, H.-G., Sommer, C.S., 2017. From magnetic SQUID prospection to excavation - investigations at Fossa Carolina, Germany. In: Jennings, B., Gaffney, C., Sparrow, T., Gaffney, S. (Eds.), 12th International Conference of Archaeological Prospection: 12th–16th September 2017. University of Bradford. Archaeopress, Oxford, pp. 144–145.
Missiaen, T., Verhegge, J., Heirman, K., Crombé, P., 2015. Potential of cone penetrating testing for mapping deeply buried palaeolandscapes in the context of archaeological surveys in polder areas. J. Archaeol. Sci. 55, 174–187. https://doi.org/10.1016/j.jas.2015.01.003.
Moskowitz, B.M., 1995. Biomineralization of magnetic minerals. Rev. Geophys. 33, 123. https://doi.org/10.1029/95RG00443.
Munsell, 1994. Munsell Soil Color Charts. 1994. Macbeth Division of Kollmorgen Instruments Corporation.
Nelson, J., 2015. Evidence in question: Dendrochronology and early medieval historians. In: Kanō, O., Lemaître, J.-L. (Eds.), Entre texte et histoire: Études d'histoire médiévale offertes au professeur Shoichi Sato. Éd. De Boccard, Paris, pp. 227–249.
Notes du général, D., 1801. 1801. Notes du général D… sur un canal qui joindrait le Rhin au Danube. Gazette nationale, ou, Le moniteur universel, pp. 624–626.
Reimer, P.J., Bard, E., Bayliss, A., Beck, J.W., Blackwell, P.G., Ramsey, C.B., Buck, C.E., Cheng, H., Edwards, R.L., Friedrich, M., Grootes, P.M., Guilderson, T.P., Haflidason, H., Hajdas, I., Hatté, C., Heaton, T.J., Hoffmann, D.L., Hogg, A.G., Hughen, K.A., Kaiser, K.F., Kromer, B., Manning, S.W., Niu, M., Reimer, R.W., Richards, D.A., Scott, E.M., Southon, J.R., Staff, R.A, Turney, C.S.M., van der Plicht, J., 2013. IntCal13 and Marine13 Radiocarbon Age Calibration Curves 0–50,000 years cal BP. Radiocarbon 55 (04), 1869–1887. https://doi.org/10.2458/azu_js_rc.55.16947.
Roberts, A.P., Chang, L., Rowan, C.J., Horng, C.-S., Florindo, F., 2011. Magnetic properties of sedimentary greigite (Fe 3 S 4): an update. Rev. Geophys. 49 (1), 1233. https://doi.org/10.1029/2010RG000336.
Saey, T., de Smedt, P., Meerschman, E., Islam, M.M., Meeuws, F., van de Vijver, E., Lehouck, A., van Meirvenne, M., 2012. Electrical Conductivity Depth Modelling with a Multireceiver EMI Sensor for Prospecting Archaeological Features. Archaeol. Prospect. 19 (1), 21–30. https://doi.org/10.1002/arp.425.
Schmidt, J., Werther, L., Zielhofer, C., 2018. Shaping pre-modern digital terrain models: the former topography at Charlemagne's canal construction site. PLoS One 13 (7), e0200167. https://doi.org/10.1371/journal.pone.0200167.
Schmidt, J., Rabiger-Völlmer, J., Werther, L., Werban, U., Dietrich, P., Berg, S., Ettel, P., Linzen, S., Stele, A., Schneider, B., Zielhofer, C., 2019. 3D-modelling of Charlemagne's Summit Canal (Southern Germany)—Merging Remote Sensing and Geoarchaeological Subsurface Data. Remote Sens. 11 (9), 1111. https://doi.org/10.3390/rs11091111.
Schmidt-Kaler, H., 1976. Geologische Karte von Bayern 7031 Treuchtlingen: 1:25 000.
Schneider, M., Stolz, R., Linzen, S., Schiffler, M., Chwala, A., Schulz, M., Dunkel, S., Meyer, H.-G., 2013. Inversion of geo-magnetic full-tensor gradiometer data. J. Appl. Geophys. 92, 57–67. https://doi.org/10.1016/j.jappgeo.2013.02.007.
Schneider, M., Linzen, S., Schiffler, M., Pohl, E., Ahrens, B., Dunkel, S., Stolz, R., Bemmann, J., Meyer, H.-G., Baumgarten, D., 2014. Inversion of Geo-magnetic SQUID Gradiometer Prospection Data using Polyhedral Model Interpretation of Elongated Anomalies. IEEE Trans. Magn. 50 (11), 1–4. https://doi.org/10.1109/TMAG.2014.2320361.
Schönfeld, G., 2009. Die altheimzeitliche Feuchtbodensiedlung von Pestenacker. Bericht der Bayerischen Bodendenkmalpflege 50, 137–156.
Schultze, V., Linzen, S., Schüler, T., Chwala, A., Stolz, R., Schulz, M., Meyer, H.-G., 2008. Rapid and sensitive magnetometer surveys of large areas using SQUIDs – the measurement system and its application to the Niederzimmern Neolithic double-ring ditch exploration. Archaeol. Prospect. 15 (2), 113–131. https://doi.org/10.1002/arp.328.
Smekalova, T.N., Yatsishina, E.B., Garipov, A.S., Pasumanskii, A.E., Ketsko, R.S., Chudin, A.V., 2016. Natural science methods in field archaeology, with the case study of Crimea. Crystallogr. Rep. 61 (4), 533–542. https://doi.org/10.1134/S1063774516030251.
Stele, A., 2017. Magnetometerprospektion und magnetische Eigenschaften von braunen Plaggeneschen (Oberesch; Lechtinger Esch) und von semiterrestrischen Sedimenten (Fossa Carolina). Dissertation. https://repositorium.ub.uni-osnabrueck.de/handle/urn:nbn:de:gbv:700-2017091916278.
Synal, H.-A., Stocker, M., Suter, M., 2007. MICADAS: a new compact radiocarbon AMS system. Nucl. Instrum. Methods Phys. Res., Sect. B 259 (1), 7–13. https://doi.org/10.1016/j.nimb.2007.01.138.
Verhegge, J., Missiaen, T., Crombé, P., 2016. Exploring Integrated Geophysics and Geotechnics as a Paleolandscape Reconstruction Tool: Archaeological Prospection of (Prehistoric) Sites buried deeply below the Scheldt Polders (NW Belgium). Archaeol. Prospect. 23 (2), 125–145. https://doi.org/10.1002/arp.1533.
Viberg, A., Trinks, I., Lidén, K., 2011. A review of the use of geophysical archaeological prospection in Sweden. Archaeol. Prospect. 18 (1), 43–56. https://doi.org/10.1002/arp.401.
Völlmer, J., Zielhofer, C., Hausmann, J., Dietrich, P., Werban, U., Schmidt, J., Werther, L., Berg, S., 2018. Minimalinvasive Direct-push-Erkundung in der Feuchtboden(geo) archäologie am Beispiel des Karlsgrabens (Fossa Carolina). Archäologisches Korrespondenzblatt 48 (4), 577–593.
Werther, L., Feiner, D., 2014. Der Karlsgraben im Fokus der Archäologie. In: Ettel, P., Daim, F., Berg-Hobohm, S., Werther, L., Zielhofer, C. (Eds.), Großbaustelle 793: Das Kanalprojekt Karls des Großen zwischen Rhein und Donau. Römisch-Germanischen Zentralmuseums, Mainz, pp. 33–40.
Werther, L., Zielhofer, C., Herzig, F., Leitholdt, E., Schneider, M., Linzen, S., Berg-Hobohm, S., Ettel, P., Kirchner, A., Dunkel, S., 2015. Häfen verbinden. Neue Befunde zu Verlauf, Wasserbaulichem Konzept und Verlandung des Karlsgrabens, in: Schmidts, T., Vucetic, M. (Eds.), Häfen im 1. Millennium AD: Bauliche Konzepte, herrschaftliche und religiöse Einflüsse. 1st ed. Schnell & Steiner, Regensburg.
Werther, L., Kröger, L., Kirchner, A., Zielhofer, C., Leitholdt, E., Schneider, M., Linzen, S., Berg-Hobohm, S., Ettel, P., 2018. Fossata Magna – A Canal Contribution to Harbour Construction in the 1st Millennium AD. In: Carnap-Bornheim, C.v., Daim, F., Ettel, P., Warnke, U. (Eds.), Harbours as Objects of Interdisciplinary Research: Archaeology + History + Geosciences. Mainz, Verlag des Römisch-Germanischen Zentralmuseums, pp. 355–370.
Weston, D.G., 2001. Alluvium and geophysical prospection. Archaeol. Prospect. 8 (4), 265–272. https://doi.org/10.1002/arp.160.
Wunderlich, T., Wilken, D., Erkul, E., Rabbel, W., Vött, A., Fischer, P., Hadler, H., Heinzelmann, M., 2018. The river harbour of Ostia Antica - stratigraphy, extent and harbour infrastructure from combined geophysical measurements and drillings. Quat. Int. 473, 55–65. https://doi.org/10.1016/j.quaint.2017.07.017.
Zielhofer, C., Kirchner, A., 2014. Naturräumliche Gunstlage der Fossa Carolina. In: Ettel, P., Daim, F., Berg-Hobohm, S., Werther, L., Zielhofer, C. (Eds.), Großbaustelle 793: Das Kanalprojekt Karls des Großen zwischen Rhein und Donau. Römisch-Germanischen Zentralmuseums, Mainz, pp. 5–8.
Zielhofer, C., Leitholdt, E., Werther, L., Stele, A., Bussmann, J., Linzen, S., Schneider, M., Meyer, C., Berg-Hobohm, S., Ettel, P., Hart, J.P., 2014. Charlemagne's Summit Canal: an early medieval Hydro-Engineering Project for Passing the central European Watershed. PLoS One 9 (9), e108194. https://doi.org/10.1371/journal.pone.0108194.
Zielhofer, C., Rabbel, W., Wunderlich, T., Vött, A., Berg, S., 2018. Integrated geophysical and (geo)archaeological explorations in wetlands. Quat. Int. 473, 1–2. https://doi.org/10.1016/j.quaint.2018.04.008.